

## FEATURE ARTICLE

## Theoretical Studies of Solute Vibrational Energy Relaxation at Liquid Interfaces

Ilan Benjamin

*Department of Chemistry and Biochemistry, University of California at Santa Cruz,  
Santa Cruz, California 95064**Received: November 7, 2005; In Final Form: January 6, 2006*

Recent advances in the theoretical understanding of solute vibrational energy relaxation at liquid interfaces and surfaces are described. Non-equilibrium molecular dynamics simulations of the relaxation of an initially excited solute molecule are combined with equilibrium force autocorrelation calculations to gain insight into the factors that influence the vibrational relaxation rate. Diatomic and triatomic nonpolar, polar, and ionic solute molecules adsorbed at the liquid/vapor interface of several liquids as well as at the water/CCl<sub>4</sub> liquid/liquid interface are considered. In general, the vibrational relaxation rate is significantly slower (a factor of 3 to 4) at the liquid/vapor and liquid/liquid interface than in the bulk due to the reduced density, which gives rise to a reduced contribution of the repulsive solvent–solute forces on the vibrational mode. The surface effects on the ionic solutes are much smaller (50% or less slower relaxation relative to the bulk). This is due to the fact that ionic solutes at the interface are able to keep part of their solvation shell to a degree that depends on their size. Thus, a significant portion of the repulsive forces is maintained. A high degree of correlation is found between the peak height of the solvent–solute radial distribution function and the vibrational relaxation rate. The relaxation rate at the liquid/liquid interface strongly depends on the location of the solute across the interface and correlates with the change in the density and polarity profile of the interface.

## I. Introduction

Over the past several decades, many experimental and theoretical studies of vibrational energy and phase relaxations in bulk liquids and at solid surfaces have been carried out. Substantial progress has been made in the development of sophisticated experimental techniques and theoretical methods. These studies have clarified the factors that are important for quantitatively understanding the rate and mechanism of vibrational relaxation in the condensed phase. While many excellent review articles have summarized these achievements,<sup>1–6</sup> this research area is still very active, both experimentally and theoretically.<sup>7–18</sup> The major motivation for the continuing interest in the problem of vibrational relaxation is its fundamental importance for the study of chemical reaction dynamics and for the insight that it provides about the nature of intermolecular interactions in complex condensed-phase systems.

The motivation for extending the vibrational relaxation studies in bulk liquids to liquid surfaces is two-fold. First, many chemical phenomena of importance in environmental science and technology take place at liquid surfaces. Examples include: phase transfer catalysis,<sup>19</sup> ion and solute transfer during solvent extraction,<sup>20</sup> and electron-transfer reactions.<sup>21,22</sup> Understanding the mechanism of vibrational relaxation is crucial for understanding the role that the liquid surface region plays in many of these reactions. Second, despite several decades of experimental and theoretical studies, some fundamental issues regarding the structure and dynamics of liquid surfaces remain open. The study of vibrational energy and phase relaxation at

liquid surfaces offers a promising way to gain insight into the nature of this complex condensed phase environment.

While the study of vibrational relaxation of adsorbates at solid surfaces has been an active area for several decades, the experimental study of vibrational dynamics at liquid surfaces (and related systems) is still in its infancy.<sup>18,23–29</sup> Owrutsky and co-workers used ultrafast transient polarization IR spectroscopy to measure the vibrational energy relaxation time of a number of pseudohalide ions (N<sub>3</sub><sup>−</sup>, NCO<sup>−</sup>, and NCS<sup>−</sup>) inside the water pools of reverse micelles.<sup>26</sup> They found relaxation times that are about three times longer in small reverse micelles compared to bulk water and suggested that this reflects the diminished hydration of the ions by water. A similar result was found for azide ion (N<sub>3</sub><sup>−</sup>) in formamide reverse micelles.<sup>18</sup> In recent years, sum frequency generation (SFG) spectroscopy has been used to measure the vibrational spectrum of molecular species at liquid interfaces,<sup>30–39</sup> and an extension of this method to the time domain has been reported at solid surfaces<sup>40–44</sup> and is being developed for liquid surfaces as well.<sup>45,46</sup>

The purpose of this article is to summarize the theoretical progress made in recent years in understanding vibrational energy and phase relaxation at liquid surfaces. The studies being reviewed include vibrational relaxation of simple diatomic and triatomic neutral, polar, and ionic solute molecules adsorbed at the liquid/vapor interface of nonpolar, polar, and hydrogen-bonding liquids and at the liquid/liquid interface. It should be stressed at the outset that the above-mentioned molecular systems were selected because they have been extensively studied theoretically and experimentally in bulk liquids, thus

enabling one to directly observe surface effects. In addition, these systems were designed to help answer some of the fundamental issues listed below. The disadvantage of this approach is that these systems may not be an ideal choice for an experimental probe at a liquid surface.

The focus of this review centers on two fundamental questions: 1. In recent years the role and interplay of electrostatic and van der Waals interactions on the vibrational energy and phase relaxation rate have been clarified.<sup>7–9,47–49</sup> How are these factors modified at the interface? 2. A decade of experimental and theoretical studies of liquid interfaces has established that the interfacial region is quite sharp even at a molecular scale and that density fluctuations give rise to a rough surface with a resulting width of 1–2 nm.<sup>50–54</sup> This, in turn, determines the length scale for variations in many molecular and macroscopic properties such as polarity,<sup>55–61</sup> hydrogen bonding strength and lifetime,<sup>62–64</sup> molecular orientations,<sup>34,62,65,66</sup> ionic distributions,<sup>50</sup> and more. How do these unique structures and dynamics manifest themselves in the rate and mechanism of vibrational relaxation?

## II. Background

There are several excellent review articles on the fundamental theory of vibrational relaxation in the condensed phase.<sup>1,4</sup> Our approach to the theoretical study of vibrational relaxation at liquid surfaces utilizes classical trajectories to (1) calculate the nonequilibrium energy correlation function starting from an initial excess energy in the solute vibration(s) and (2) calculate equilibrium force correlation functions which can be used to determine the rate and mechanism of the relaxation based on a simple semiclassical perturbation theory.<sup>1</sup>

**1. Non-equilibrium Studies.** Non-equilibrium vibrational energy relaxation dynamics are studied by averaging the vibrational energy of the solute molecule in hundreds of independent trajectories. In each trajectory, the solute is prepared with an initial vibrational energy,  $E(0)$ , that is significantly larger than the classical equilibrium value of  $kT$  per vibrational mode. The coordinate and velocity distributions of the initial conditions of all other solute and solvent modes follow the Boltzmann distribution at the temperature  $T$  (typically 298 K). Each trajectory is run in a constant energy ensemble for a period of a few tens of picoseconds, depending on the system studied. The trajectories are averaged to obtain the normalized non-equilibrium correlation function:<sup>67</sup>

$$C(t) = \frac{\bar{E}(t) - \bar{E}(\infty)}{\bar{E}(0) - \bar{E}(\infty)} \quad (1)$$

where  $\bar{E}(t)$  is the average vibrational energy of the solute (or of one of the vibrational modes in the case of a polyatomic molecule) at time  $t$ , and  $\bar{E}(\infty) \approx kT$  is the final equilibrium energy (per mode). Typically, this procedure is repeated for the

Ilan Benjamin was born in Israel in 1956. He received his B.Sc. in chemistry and physics from the Hebrew University of Jerusalem in 1982 and his Ph.D. in theoretical chemistry in 1986, working under the direction of Professor Raphael Levine at the Hebrew University of Jerusalem. He was a Weizmann Postdoctoral Fellow at the University of Pennsylvania and also held a postdoctoral position at the University of California at San Diego. In 1989, he joined the faculty at the University of California at Santa Cruz, where he is currently a professor of physical chemistry. In 1995–1996, he was a visiting professor at the Weizmann Institute of Science, Israel. Benjamin's research interests include the theoretical and computational studies of relaxation processes and chemical reaction dynamics in the condensed phase. In recent years, his research has focused on chemical reactions and molecular interactions at liquid interfaces.

different interfacial systems and when the solute is located in the bulk. If  $C(t)$  is well approximated by a single exponential, one can obtain the lifetime  $\tau_{\text{NE}}$  from the fit:  $C(t) = e^{-t/\tau_{\text{NE}}}$ ; otherwise an average lifetime may be calculated using:  $\tau_{\text{NE}} = \int_0^\infty C(t) dt$ .

**2. Equilibrium Perturbative Approach.** This approach is based on the Fermi golden rule,<sup>1</sup> where the quantum relaxation rate of a vibrational mode coupled to a bath is approximated as the Fourier transform of a force correlation function, which in turn is approximated using classical trajectories. This method has been extensively used in recent years to calculate vibrational relaxation rates of diatomic and polyatomic solutes in liquids.<sup>7,8,10,11,68,69</sup>

The implementation of this method involves long (on the order of 1 ns) equilibrium (constant temperature) trajectories, in which the solute molecule's vibrational coordinate is held fixed at its equilibrium value (using SHAKE, or similar, algorithms<sup>70</sup>). During the trajectory, the force on the vibrational coordinate is determined and used in the computation of the fluctuating force power spectra. In the case of a diatomic solute, if  $\mathbf{F}_A$  and  $\mathbf{F}_B$  are the total forces on the two solute atoms, one obtains<sup>47,71</sup>

$$\zeta(\omega) = \int_{-\infty}^{\infty} \langle \delta F(t) \delta F(0) \rangle \cos(\omega t) dt \quad (2)$$

where,

$$\delta F(t) = F(t) - \langle F \rangle, F = \mu(\mathbf{F}_A/m_A - \mathbf{F}_B/m_B) \cdot \mathbf{n}_{AB} \quad (3)$$

and where  $\langle \dots \rangle$  denotes an equilibrium ensemble average, and  $\mathbf{n}_{AB}$  is a unit vector in the direction of the diatomic bond.

If the vibrational relaxation problem is modeled as a classical harmonic oscillator linearly coupled to a bath, then the power spectrum of the fluctuating force can be used to calculate the relaxation rate using the Landau–Teller formula:<sup>1,71,72</sup>

$$\tau_{\text{LT}} = \mu kT / \zeta(\omega_{\text{eq}}) \quad (4)$$

where  $\omega_{\text{eq}}$  is the equilibrium oscillator frequency (which may be shifted relative to the gas-phase value  $\omega_0$ ). The Landau–Teller result is a reasonable approximation for low-frequency vibrations at high temperatures. Bader and Berne<sup>73</sup> and Skinner<sup>74</sup> have shown that the exact quantum energy relaxation rate for a harmonic oscillator coupled to a harmonic bath is identical to the classical result if the classical power spectrum (eq 2) is multiplied by the quantum correction factor  $\beta \hbar \omega / (1 - e^{-\beta \hbar \omega})$ .

The classical power spectra may be used to gain insight into the nature of the intermolecular interactions contributing to the relaxation. This can be done by computing different components of the force power spectra. For example, one may write the fluctuation in the total force  $\delta F = F - \langle F \rangle$  as a sum of contributions from electrostatic and non-electrostatic (Lennard-Jones) terms:  $\delta F = \delta F_{\text{el}} + \delta F_{\text{LJ}}$ . The total force autocorrelation function has the following contributions:

$$\begin{aligned} \langle \delta F(t) \delta F(0) \rangle &= \langle \delta F_{\text{el}}(t) \delta F_{\text{el}}(0) \rangle + \langle \delta F_{\text{LJ}}(t) \delta F_{\text{LJ}}(0) \rangle + \\ &\quad \langle \delta F_{\text{el}}(t) \delta F_{\text{LJ}}(0) \rangle + \langle \delta F_{\text{LJ}}(t) \delta F_{\text{el}}(0) \rangle \end{aligned} \quad (5)$$

As a result, the power spectrum can be written as a sum of contributions due to the fluctuating electrostatic forces ( $\zeta_{\text{el}}(\omega)$ ), Lennard-Jones forces ( $\zeta_{\text{LJ}}(\omega)$ ), and the cross term ( $\zeta_{\text{cross}}(\omega)$ ):

$$\zeta(\omega) = \zeta_{\text{el}}(\omega) + \zeta_{\text{LJ}}(\omega) + \zeta_{\text{cross}}(\omega) \quad (6)$$

In the case of a solute located at the interface between two

**TABLE 1: Morse Potential Parameters for Several Diatomic Solutes Examined in This Work**

molecule	$D_e$ (kcal/mol)	$R_{eq}$ (Å)	$\alpha$ (Å <sup>-1</sup> )	$\omega_{eq}$ (cm <sup>-1</sup> )
I <sub>2</sub>	36.4	2.67	1.84	215
I <sub>2</sub> <sup>-</sup>	25.4	3.23	1.16	113
OC1	63.4	1.59	2.328	870
OC1 <sup>-</sup>	51.4	1.67	2.148	713

liquids such as water and oil, one may similarly write the total power spectrum as a sum of the contribution from the water and the oil molecules and the cross term:

$$\zeta(\omega) = \zeta_w(\omega) + \zeta_o(\omega) + \zeta_{wo}(\omega) \quad (7)$$

All the molecular dynamics simulations described below were carried out using a time step of 0.5 fs and the velocity version of the Verlet algorithm.<sup>75</sup>

**3. Systems and Potentials.** The systems studied all included one solute molecule (diatomic or triatomic) adsorbed at a liquid/vapor interface or at the interface between two immiscible liquids. In every case, calculations in the bulk of the relevant liquid(s) were performed for comparison. In some cases, to increase sampling statistics, the solute molecule's center of mass was restricted to a 3 Å-wide slab parallel to the interface by a harmonic potential, which was zero whenever the solute was inside the slab. The diatomic solute was typically modeled using the anharmonic Morse potential:

$$V(R) = D_e [e^{-\alpha(R - R_{eq})} - 1]^2 \quad (8)$$

The parameters  $D_e$ ,  $\alpha$ , and  $R_{eq}$  for the several diatomic solute molecules discussed in this paper are listed in Table 1, together with their fundamental gas-phase vibrational frequency  $\omega_0$ . Many of the calculations were performed on I<sub>2</sub> and I<sub>2</sub><sup>-</sup> due to the fact that these molecules have been extensively studied in bulk liquids, both experimentally<sup>76–78</sup> and theoretically.<sup>79,80</sup> In addition, the low-frequency vibration of the I–I bond in these two molecules gives some justification for the use of classical mechanics in the non-equilibrium relaxation calculations.

The liquid molecules occupied a rectangular box of dimension  $L_x \times L_y \times L_z$ , with  $L_x = L_y < L_z$  such that the flat interface is perpendicular to the long Z-axis of the simulation box. The Gibbs dividing surface (where the density of one of the liquids is 50% of the bulk value<sup>81</sup>) is taken to be at  $Z = 0$ . Periodic boundary conditions were used in all three dimensions with a molecule-based force-switching function at  $L_x/2$ . In some cases, system size dependence was examined<sup>82</sup> and found to be insignificant.

The liquid intermolecular potentials follow the standard choice of pairwise additive atom-based Lennard-Jones plus Coulomb terms:

$$u_{ij}(r) = 4\epsilon_{ij} \left[ \left( \frac{\sigma_{ij}}{r} \right)^{12} - \left( \frac{\sigma_{ij}}{r} \right)^6 \right] + \frac{q_i q_j}{4\pi r \epsilon_0} \quad (9)$$

where “ $i$ ” and “ $j$ ” denote atoms on two different molecules separated by a distance  $r$ . The Lennard-Jones parameters and the charges for the individual atomic sites in the different liquids used in this work can be found elsewhere.<sup>82–88</sup> The Lennard-Jones parameters for the interactions between different atom types are determined from the standard (Lorentz–Berthelot) mixing rules.<sup>89</sup>

$$\sigma_{ij} = (\sigma_{ii} + \sigma_{jj})/2, \quad \epsilon_{ij} = (\epsilon_{ii}\epsilon_{jj})^{1/2} \quad (10)$$

Given the large amount of vibrational energy dissipation in the

**TABLE 2: Calculated Vibrational Relaxation Lifetime of Different Solute Molecules at the Liquid/Vapor Interface of Several Solvents at 298 K**

solute	solvent	bulk lifetime (ps)	liquid/vapor lifetime (ps)	reference
I <sub>2</sub> <sup>-</sup>	H <sub>2</sub> O	0.60	0.90	84
I <sub>2</sub>	H <sub>2</sub> O	5.4	16.6	84
C1O	H <sub>2</sub> O	7.9	28.2	87
C1O <sup>-</sup>	H <sub>2</sub> O	0.64	0.69	87
C1O	CH <sub>3</sub> CN	179	555	87
C1O <sup>-</sup>	CH <sub>3</sub> CN	13.9	14.3	87
ICN	H <sub>2</sub> O	0.72	1.75	88
ICN	CHCl <sub>3</sub>	14.3	46	85
OC1O	H <sub>2</sub> O	6.4	11.6	86
OC1O	CH <sub>3</sub> CN	31.9	55.6	86
OC1O	C <sub>2</sub> H <sub>5</sub> OH	30.4	41.7	86

non-equilibrium calculations, in all cases we opted to use fully flexible liquid intramolecular potentials. For water, we selected a power series potential fitted to spectroscopic data.<sup>90</sup> The intramolecular potential energy function for other liquids typically included harmonic bond stretching and angle bending and, when applicable, cosine series for the torsional modes. All the liquid models used give reasonable bulk and interfacial properties, as demonstrated elsewhere.<sup>91,92</sup>

A comment about the intermolecular potential energy functions used in this work: In every case, these potentials are pairwise additive, so that the polarizable nature of the solvent and solute molecules is effectively introduced by proper adjustment of the Lennard-Jones parameters and the partial charges on the individual solvent and solute atomic sites. In recent years, the effect of many-body polarizable potentials on the structure and dynamics of condensed bulk<sup>93–100</sup> and interfacial inhomogeneous systems<sup>101–107</sup> has been the subject of many studies. The above references show that in some cases these potentials seem to make only a small contribution, and in other cases they have been shown to have an important effect. Although there are indications that dynamic solute polarizabilities could accelerate the rate of vibrational relaxation in bulk liquids,<sup>99,108,109</sup> the role of dynamic solvent polarizability remains an issue for future studies.

### III. Results and Discussion

**1. Vibrational Energy Relaxation at the Liquid/Vapor Interface.** Vibrational energy relaxation rates  $k_{VER}$  (or lifetimes:  $\tau = 1/k_{VER}$ ) were determined by nonequilibrium trajectories according to the procedure outlined in section II.1. The resulting nonequilibrium correlation functions can sometimes be fit to a single exponential function. This is typically the case where, in the range of the excess vibration energy considered, the relaxation rate is only weakly dependent on the excitation energy. If the relaxation rate is strongly dependent on the excitation energy (which is typically the case when the fundamental vibrational frequency is much larger than  $kT/h$ ), then one may report the average vibrational lifetime given by  $\tau_{NE} = \int_0^\infty C(t) dt$ . The results for all the liquid/vapor interface systems studied are given in Table 2, together with the bulk results.

All calculated lifetimes in the bulk are in good to excellent agreement with experiments (see the indicated references for details and for references to the experimental data).

We note that in all cases the bulk lifetime is shorter than the interfacial one. Neutral (polar or nonpolar) diatomic molecules in polar liquids experience a factor of 3.1–3.5 slower relaxation at the liquid/vapor interface than in the bulk. The ionic solutes behave differently: I<sub>2</sub><sup>-</sup> shows a slower relaxation (at the interface



vs the bulk) by a factor of 1.5 while,  $\text{ClO}^-$  vibrational relaxation at the interface is almost identical to that in the bulk (for both solvents studied). The average relaxation rate of the bending and C–N stretching modes of ICN slows down by a factor of 3.2 in  $\text{CHCl}_3$  and 2.4 in water, while the total vibrational energy of OCIO at the interface is a factor of 1.4–1.8 slower than in the bulk.

To understand why the surface effect in the case of ionic diatomic molecules is significantly less pronounced than in the case of neutral molecules, one needs to understand the contribution of electrostatic interactions to the rate of vibrational relaxation in polar liquids. This topic has been the subject of a number of theoretical and computational studies in bulk liquids,<sup>8,9,47–49</sup> motivated by experimental findings of a significant enhancement in the vibrational energy relaxation rate of ionic solutes compared with a similar neutral solute.<sup>3,77,110,111</sup> The main conclusion of these studies that is relevant to our topic here was summarized by Ladanyi and Stratt:<sup>49</sup> The vibrational relaxation is dominated by the short-range repulsive forces even for an ionic solute in a highly polar solvent. The role of the Coulombic forces is to order the solvent molecules around the solute, so that the repulsive forces are amplified. This conclusion was supported by a study of diatomic solutes of varying polarity in  $\text{CH}_3\text{CN}$  and  $\text{CO}_2$  solvents.

A simple analysis of a one-dimensional Lennard-Jones plus Coulomb potential can be used to demonstrate this idea (referred to as electrostriction). Consider the pair interaction between a solute atom with a charge of 0 or 1 and a solvent atom with a charge of  $q$ . For simplicity of notation, we drop the  $i$  and  $j$  indices from eq 9, and thus consider

$$u(r) = 4\epsilon \left[ \left( \frac{\sigma}{r} \right)^{12} - \left( \frac{\sigma}{r} \right)^6 \right] + \frac{q}{4\pi r \epsilon_0} \quad (11)$$

This term is representative of the different contributions to the total force along the vibrating bond. Since the vibrational relaxation of the solute is a result of the fluctuations in the total force along the bond,  $f = -du/dr$ . While the exact relaxation depends on the Fourier component of the fluctuating force at the oscillator frequency (as will be shown below), the mean square deviation:  $\sigma_f = \langle (f - \langle f \rangle)^2 \rangle$  (where  $\langle \dots \rangle$  represents a Boltzmann averaging at a temperature  $T$ ) gives a qualitative indication of the overall magnitude of the fluctuations in the force at zero frequency. This can be easily calculated numerically, and the results are shown in Figure 1 as a function of the dimensionless parameter  $\chi$  defined as:  $\chi = q/(4\pi\epsilon_0\sigma\epsilon)$ , which gives the relative strength of the electrostatic interactions. Figure 1 demonstrates that while the electrostatic interactions make the major contribution to the average force, fluctuations in the force are dominated by short-range Lennard-Jones interactions. Note that the contribution of the Lennard-Jones interactions to  $\sigma_f$  increases with the increase in the strength of the electrostatic interactions. As discussed by Ladanyi and Stratt, the increase in the electrostatic interactions brings the equilibrium position (the point at which  $f = 0$ ) higher on the repulsive part of the Lennard-Jones potential, so that small fluctuations in  $r$  result in large variations in the Lennard-Jones force, while the slowly varying Coulomb forces make a much smaller contribution.

This simple one-dimensional model can help with the interpretation of the equilibrium force power spectra and the related frequency-dependent friction on the vibrational mode. As an example, consider the case of  $\text{I}_2^-$  and  $\text{I}_2$  in bulk water versus at the water/liquid vapor interface. The frequency-dependent friction,  $\zeta(\omega)/\mu kT$ , in the region  $\omega = 100\text{--}250\text{ cm}^{-1}$  is a monotonically decreasing function. The inverse of this

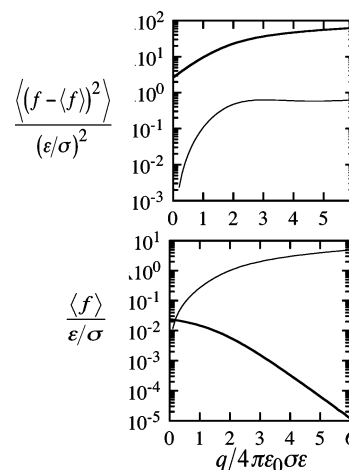


**Figure 1.** Mean square deviation (top panel) and average force (bottom panel) for the Lennard-Jones (solid line) and electrostatic (dashed line) force components of a one-dimensional model (eq 11) as a function of a dimensionless parameter  $\chi = q/(4\pi\epsilon_0\sigma\epsilon)$ .

**TABLE 3: Landau-Teller Vibrational Lifetimes in Bulk Water and at the Water Liquid/Vapor Interface**

solute molecule (in water)	$\tau_{\text{LT}}$ bulk (ps)	$\tau_{\text{LT}}$ interface (ps)
$\text{I}_2^-$	0.6	0.8
$\text{I}_2$	4.6	21.2
$\text{I}_2^-$ (215 $\text{cm}^{-1}$ ) <sup>a</sup>	1.3	1.8
$\text{I}_2$ (113 $\text{cm}^{-1}$ ) <sup>b</sup>	1.4	5.5

<sup>a</sup> A fictitious  $\text{I}_2^-$  molecule (interacts with the solvent as  $\text{I}_2^-$ ) with the vibrational frequency of the  $\text{I}_2$  oscillator. <sup>b</sup> A fictitious  $\text{I}_2$  molecule (interacts with the solvent as  $\text{I}_2$ ) with the vibrational frequency of the  $\text{I}_2^-$  oscillator.

function at the oscillator frequency is the Landau–Teller approximation of the vibrational lifetime,  $\tau_{\text{LT}}$ . Comparing the friction for  $\text{I}_2$  in bulk water to the friction at the water/liquid vapor interface shows that the interfacial friction is significantly lower than the one in the bulk, corresponding to a three times slower relaxation at the interface than in the bulk. In contrast, for  $\text{I}_2^-$  the friction at the interface is only slightly lower than the one in the bulk, corresponding to the slightly slower relaxation at the interface compared to in the bulk. This is just what was found when the non-equilibrium lifetimes were discussed, and Table 3 quantifies this by presenting the Landau–Teller lifetimes. This table also gives the predicted lifetime for the fictitious  $\text{I}_2^-$  molecule with the vibrational frequency of the  $\text{I}_2$  oscillator (215  $\text{cm}^{-1}$ ) as well as the predicted lifetime for the fictitious  $\text{I}_2$  molecule at the frequency of the  $\text{I}_2^-$  oscillator (113  $\text{cm}^{-1}$ ). This shows that the total friction on the  $\text{I}_2^-$  bond at the interface is  $21.2/1.8 \approx 12$  times larger than that on  $\text{I}_2$  at the same frequency, while in the bulk it is larger by a factor of  $4.6/1.3 = 3.5$ . By further examining the contribution of the electrostatic friction to the total friction, one finds that for  $\text{I}_2^-$  both in bulk water and at the interface, the electrostatic friction makes a negligible contribution to the total friction.<sup>84</sup>

What accounts for the fact that the relaxation of the ionic oscillator at the interface is so similar to the relaxation in the bulk and so much faster than that of the nonionic molecule, despite the fact that the electrostatic friction contributes so little to the total friction? The one-dimensional model discussed above offers a simple explanation, which is also consistent with the insight gained from the work of Ladanyi and Stratt:<sup>49</sup> As mentioned before, the attractive solute–solvent electrostatic forces put the solute–solvent equilibrium distance on the repulsive side on the Lennard-Jones potential, which causes large fluctuations in the force and thus an increased friction on the

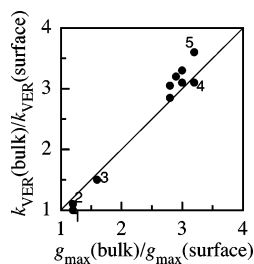


**Figure 2.** Surface effect on the vibrational rate versus surface effect on the height of the first peak of the solute–solvent radial distribution function. Points labeled 1–5 correspond to different diatomic solute systems at the liquid/vapor interface: (1)  $\text{ClO}^-/\text{H}_2\text{O}$ ; (2)  $\text{ClO}^-/\text{CH}_3\text{CN}$ ; (3)  $\text{I}_2^-/\text{H}_2\text{O}$ ; (4)  $\text{I}_2/\text{H}_2\text{O}$ ; (5)  $\text{ClO}/\text{H}_2\text{O}$ . Other points correspond to all other systems listed in Table 2, as explained in the text.

vibrational coordinate. Previous studies by us and others<sup>62,112</sup> have demonstrated that an ionic solute at the liquid/vapor interface tends to keep its hydration structure similar to the bulk in terms of the location and height of the first peak of the solute–solvent radial distribution function. This effect is more pronounced as the ionic solute becomes smaller in size. Putting all this together suggests that as an ionic solute is moved to the interface, its ability to keep its hydration shell enables the Lennard-Jones component of the friction to remain nearly intact. In contrast, as a nonionic (even polar) solute is moved to the interface, a marked decrease in its hydration shell leads to a diminished Lennard-Jones component of the friction, and thus a significant decrease in the vibrational relaxation rate. A clear demonstration of the correlation between the robustness of the hydration shell and the surface effect on the rate is given in Figure 2, in which the ratio of the bulk-to-surface vibrational rate is plotted against the ratio of the peak height of the solute–solvent radial distribution function. Each point corresponds to one of the molecular systems studied in the bulk and at the liquid/vapor interface. Most of the points lie directly near the line  $y = x$ . The cluster near the origin (bulk to surface rate ratio near 1), where surface effect is minimal, corresponds to ionic compounds, and the cluster of points near the point of bulk-to-surface rate ratio of 3 corresponds to nonionic compounds.

**2. Vibrational Energy Relaxation at the Liquid/Liquid Interface.** The fundamental reason for the reduction in the vibrational relaxation rate at the liquid/vapor interface for nonionic solutes is the reduced solvent density, which reduces the average number of solvent molecules at the first solvation shell. Indeed, if the local (rather than the bulk) solvent density is used to normalize the solvent–solute pair correlation function, the first peak at the interface and in the bulk are almost the same.<sup>84,87</sup> The reduced total solvent neighbors reduce the strength of the repulsive part of the Lennard-Jones solute–solvent forces and lead to a longer lifetime. Ionic solutes interfere with this trend by keeping a larger part of the first solvation shell and thus increasing the local density relative to the average interface region. This phenomenon is referred to as electrostriction.

At the interface between two immiscible liquids, the *total* density variation is much less pronounced, and the key property that varies across the interface is the effective polarity, which broadly speaking characterizes the ability of polar solvent(s) to interact favorably with the solute.<sup>113</sup> Molecular dynamics simulations,<sup>57,58</sup> theoretical calculations,<sup>114</sup> and experiments<sup>55,56,59–61</sup> suggest that the polarity varies from the bulk value of one liquid to the value at the bulk of the second liquid over a distance of a few nanometers. The other important characteristics of liquid/liquid interfaces, as suggested by molecular dynamics simulations<sup>50,51,53</sup> and experiments,<sup>52,54,115</sup>

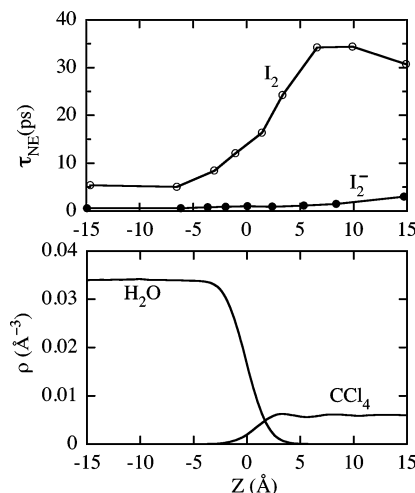


**Figure 3.** Top panel: non-equilibrium vibrational relaxation time for  $\text{I}_2$  and  $\text{I}_2^-$  adsorbed at different locations at the water/ $\text{CCl}_4$  interface. Each point is obtained from an average over 500 trajectories, as explained in the text. Bottom panel: density profiles of the two liquids. Data taken from ref 82.

is that the apparent width of the interface is the result of thermally excited nanometer scale capillary waves giving rise to a dynamically rough surface.

The solute molecules examined at the liquid/vapor interface were molecules that adsorbed at the liquid/vapor interface, and their location was simply selected to correspond to the location of the free energy minimum. One of the goals of extending the vibrational relaxation studies to the liquid/liquid interface has been to investigate the depth profile of this region. The other goal has been the examination of the generality of the argument about correlation between the solvation structure and the vibrational lifetime made above in the liquid/vapor interface studies.

With these goals in mind, the vibrational relaxation of  $\text{I}_2^-$  and  $\text{I}_2$  at different locations across the water/ $\text{CCl}_4$  liquid/liquid interface has been studied.<sup>82</sup> Figure 3 (top panel) depicts the vibrational lifetime calculated for seven different surface locations of these two solute molecules. The “ $y$ ” coordinate of each point on this plot was obtained by fitting a single exponential to 500 nonequilibrium energy relaxation trajectories of 10 ps each. The large number of trajectories used in the determination of each point gives rise to the relatively small statistical error of 3% to 5%. The “ $x$ ” coordinate corresponds to the average location of the solute center of mass during these trajectories. The initial  $z$  position of the solute in these trajectories was selected from a distribution where the solute was constrained to a 3 Å-wide slab parallel to the interface, so the seven interfacial locations correspond to an overlapping sequence of these windows from the bulk water region to the bulk  $\text{CCl}_4$  region. The density profiles of the two liquids are also shown (bottom panel), where  $Z = 0$  is the approximate location of the Gibbs dividing surface,<sup>81</sup> which approximately corresponds to the plane where the water density is near 50% of the bulk value.

As the solutes are moved from bulk water to bulk  $\text{CCl}_4$ , the relaxation time increases monotonically for both the ionic and nonionic solute. However, while the relaxation time for  $\text{I}_2$  varies from 5 ps in bulk water to around 30 ps in bulk  $\text{CCl}_4$  in a nearly uniform fashion across the interface, the relaxation time of  $\text{I}_2^-$  shows little variation as the  $\text{I}_2^-$  moves across the interface, with most of the change taking place just as the solute arrives in the bulk organic region. This behavior approximately tracks the change in the density profile of the two liquids, but a more

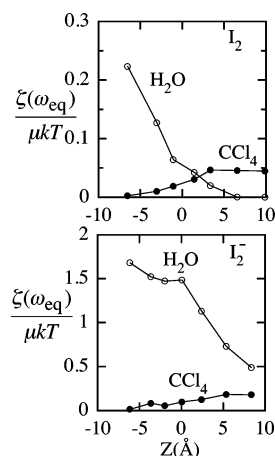


**Figure 4.** The contribution of water and  $\text{CCl}_4$  to the frequency-dependent friction on the  $\text{I}_2$  (top panel) and  $\text{I}_2^-$  (bottom panel) bonds as a function of location at the water/ $\text{CCl}_4$  liquid/liquid interface. Data taken from ref 82.

exact correlation with the hydration structure will be discussed below. Note that recent experiments showing a slowing down of vibrational relaxation rate as the water content of reverse micelles is reduced<sup>25</sup> are clearly related to this behavior.

The fundamental reason for the marked difference between the behavior of the ionic and nonionic solutes can be related to the electrostriction effect discussed in the previous section. First, note that the relaxation of the nonpolar solute in bulk water is faster than in bulk  $\text{CCl}_4$  due to the larger density of phonon states in water in the region of the oscillator frequency. This is evident from a comparison of the frequency-dependent friction  $\zeta(\omega)/\mu kT$  as a function of  $\omega$  in the two bulk liquids.<sup>82</sup> As the nonionic solute is transferred from water to bulk  $\text{CCl}_4$ , the number of water molecules in the first hydration shell decreases monotonically with a corresponding decrease in the friction on the I–I bond, giving rise to an increase in the vibrational lifetime. The ionic solute vibrational relaxation is also faster in bulk water than in bulk  $\text{CCl}_4$  for a similar reason, but also because the electrostatic forces pull the water molecules tighter around the solute and produce an increase in the Lennard-Jones component of the friction. As the ionic solute is transferred to the organic phase across the interface, the ability of the electrostatic forces to keep the hydration shell intact for a longer distance gives rise to almost unchanged Lennard-Jones friction, and thus the rate variation across the interface is much less pronounced. Figure 4 confirms this picture by showing the contribution of the water and  $\text{CCl}_4$  to the total friction: The contribution of  $\text{CCl}_4$  to the friction on the I–I bond in the ionic and the nonionic solute is very similar. The water contribution, which is much smaller in the case of the nonionic solute, drops immediately and sharply as the solute crosses the interface, while in the ionic case (much larger friction) the change in friction, as the solute begins to cross the interface, is relatively small. As in the case of vibrational relaxation at the liquid/vapor interface, most of the contribution to the friction comes from the Lennard-Jones component of the force.<sup>82</sup> As discussed before, this manifests itself in the high correlation found at the liquid/vapor interface case between the height of the first peak of the solvent–solute radial distribution function and the vibrational relaxation rate. The same correlation was found here.<sup>82</sup>

The ability of the ionic solute to maintain a partial hydration shell as it crosses the interface (and in the case of a very small solute, to even keep it all the way to the bulk organic phase) gives rise to unique liquid/liquid interface structural effects.

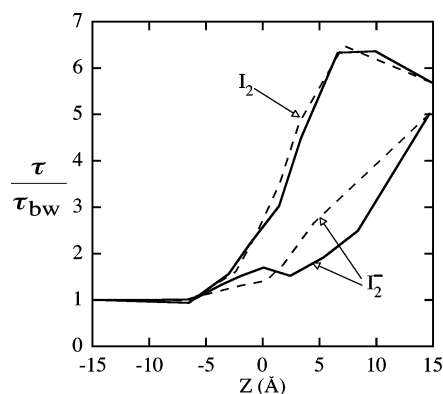


**Figure 5.** Vibrational relaxation time relative to bulk water for  $\text{I}_2$  and  $\text{I}_2^-$  at the normal water/ $\text{CCl}_4$  liquid/liquid interface (solid line) and at an externally constrained interface in which density fluctuations normal to the interface are suppressed (dashed line).

These are closely related to the normal dynamic roughness observed at the neat liquid/liquid interface. They have been previously demonstrated by examining the water surface excess as a function of solute location.<sup>82,116</sup> Another way to demonstrate this effect is as follows: The calculations discussed above on the non-equilibrium and equilibrium studies of  $\text{I}_2$  and  $\text{I}_2^-$  at the (normal) water/ $\text{CCl}_4$  interface are repeated on a modified system in which the interface is forced to remain molecularly sharp and flat by a small external potential that suppresses the natural thermal roughness of the interface.

Figure 5 presents the non-equilibrium vibrational lifetime as a function of the solutes' location, calculated with the constraint interface structure (dashed lines) compared with the normal interface results presented earlier. No change is observed for the case of the neutral solute, suggesting no significant modification of the interface structure when the solute crosses the interface. However, the relaxation time of the ionic solute rises significantly more in the case of the constrained interface compared with the normal interface. This suggests that the deformation of the interface structure when the ionic solute crosses the normal (unconstrained) interface is an important aspect of the slow rise of the vibrational lifetime in that case.

#### IV. Conclusions and Outlook

In the case of nonionic (polar or nonpolar) solutes, the relaxation rate at the interface is slowed significantly relative to the bulk (by a factor of 3–4) due to the reduction in density and the corresponding reduction in vibrational friction. In contrast, the relaxation rate of ionic solutes is slowed by only about 50%, and the effect almost disappears for a small ionic solute.<sup>87</sup> It was demonstrated that this is due to the ability of ionic solutes (especially small ones) to keep their solvation shells almost intact and thus maintain almost the same level of vibrational friction. Consistent with this interpretation is the high degree of correlation found between the relaxation rate and the peak of the solvent–solute orientationally averaged interfacial radial distribution function. The above results are consistent with a study by Ladanyi and Strat,<sup>9,49</sup> who showed that the solvent–solute electrostatic forces provide the equilibrium structure that enables the Lennard-Jones forces in the first solvation shell to make the major contribution to the friction.

These results seem quite general, as similar observations were found in the case of triatomic solutes. However, in this case, intramolecular energy flow is an important new aspect that may contribute to the overall rate and the relaxation mechanism. An important issue that remains open to future studies is the



interface effect on the rate of intramolecular energy flow between the solute vibrational modes.

Another important issue that has been only briefly studied thus far is liquid surface effects on frequency shift and vibrational dephasing time, a problem that has attracted a lot of attention in bulk liquids.<sup>8,117–128</sup> Preliminary results<sup>82</sup> on frequency shifts of I<sub>2</sub> and I<sub>2</sub><sup>−</sup> at the water/CCl<sub>4</sub> interface show that the strong blue shift in the vibrational frequency of the ionic solute and its variation with location across the interface are consistent with the partial preservation of the hydration shell as the solute crosses the interface. This is in agreement with several studies in bulk liquids, which show that the blue shift observed for the ionic solute and the very small shift in the case of the neutral solute are consistent with the dominance of the repulsive contributions to the average force on the vibrational coordinate.<sup>8,110</sup> On the other hand, since the pure dephasing time depends mainly on contributions from the harmonic (linear) component of both the Lennard-Jones and Coulomb forces, its variation across the interface is not marked.<sup>82</sup>

While the work reviewed above has identified some of the important factors that influence the vibrational relaxation of solute molecules adsorbed at liquid interfaces, much more remains to be done. On the theoretical front, more studies are needed, especially in the area of vibrational dephasing, polyatomic solutes, and the role of polarizable solvent and solute forces. Experimental work on some specific systems where the polarity of the solvent, the solute size and charge are varied will be necessary to test the ideas discussed above.

**Acknowledgment.** This work has been supported by a grant from the National Science Foundation (CHE-0345361).

## References and Notes

- Oxtoby, D. W. *Adv. Chem. Phys.* **1981**, 47, 487.
- Chesnoy, J.; Gale, G. M. *Adv. Chem. Phys.* **1988**, 70(part 2), 297.
- Owrutsky, J. C.; Raftery, D.; Hochstrasser, R. M. *Annu. Rev. Phys. Chem.* **1994**, 45, 519.
- Stratt, R. M.; Maroncelli, M. *J. Phys. Chem.* **1996**, 100, 12981.
- Heilweil, E. J.; Casassa, M. P.; Cavanagh, R. R.; Stephenson, J. C. *Annu. Rev. Phys. Chem.* **1989**, 40, 143.
- Tully, J. C. *Annu. Rev. Phys. Chem.* **2000**, 51, 153.
- Rey, R.; Hynes, J. T. *J. Chem. Phys.* **1996**, 104, 2356.
- Rey, R.; Hynes, J. T. *J. Chem. Phys.* **1998**, 108, 142.
- Ladanyi, B. M.; Stratt, R. M. *J. Phys. Chem. A* **1998**, 102, 1068.
- Egorov, S. A.; Skinner, J. L. *J. Chem. Phys.* **1996**, 105, 7047.
- Egorov, S. A.; Skinner, J. L. *J. Chem. Phys.* **2000**, 112, 275.
- Lawrence, C. P.; Skinner, J. L. *J. Chem. Phys.* **2002**, 117, 5827.
- Lawrence, C. P.; Skinner, J. L. *J. Chem. Phys.* **2003**, 119, 1623.
- Coalson, R. D.; Evans, D. G. *Chem. Phys.* **2004**, 296, 117.
- Bakker, H. J. *J. Chem. Phys.* **2004**, 121, 10088.
- Ma, A.; Stratt, R. M. *J. Chem. Phys.* **2004**, 121, 11217.
- Bolinger, J. C.; Bixby, T. J.; Reid, P. J. *J. Chem. Phys.* **2005**, 123, 1623.
- Sando, G. M.; Dahl, K.; Zhong, Q.; Owrutsky, J. C. *J. Phys. Chem. A* **2005**, 109, 5788.
- Interfacial Catalysis*; Volkov, A. G., Ed.; Marcel Dekker: New York, 2003.
- Solvent Extraction for the 21st Century*; Cox, M.; Hidalgo, M.; Valiente, M., Eds.; SCI: London, 2001.
- Vanysek, P. *Electrochim. Acta* **1995**, 40, 2841.
- Liquid-Liquid Interfaces*; Volkov, A. G.; Deamer, D. W., Eds.; CRC Press: Boca Raton, 1996.
- Yi, J.; Jonas, J. *J. Phys. Chem.* **1996**, 100, 16789.
- Matranga, C.; Guyot-Sionnest, P. *J. Chem. Phys.* **2000**, 112, 7615.
- Zhong, Q.; Baronavski, A. P.; Owrutsky, J. C. *J. Chem. Phys.* **2003**, 118, 7074.
- Zhong, Q.; Baronavski, A. P.; Owrutsky, J. C. *J. Chem. Phys.* **2003**, 119, 9171.
- Kalampounias, A. G.; Yannopoulos, S. N.; Steffen, W.; Kirillova, L. I.; Kirillov, S. A. *J. Chem. Phys.* **2003**, 118, 8340.
- Li, S. M.; Shepherd, T. D.; Thompson, W. H. *J. Phys. Chem. A* **2004**, 108, 7347.
- Dokter, A. M.; Woutersen, S.; Bakker, H. J. *Phys. Rev. Lett.* **2005**, 94, 178301.
- Zhang, D.; Gutow, J. H.; Eisenthal, K. B.; Heinz, T. F. *J. Chem. Phys.* **1993**, 98, 5099.
- Du, Q.; Superfine, R.; Freysz, E.; Shen, Y. R. *Phys. Rev. Lett.* **1993**, 70, 2313.
- Du, Q.; Freysz, E.; Shen, Y. R. *Science* **1994**, 264, 826.
- Baldelli, S.; Schnitzer, C.; Shultz, M. J. *J. Chem. Phys.* **1998**, 108, 9817.
- Miranda, P. B.; Shen, Y. R. *J. Phys. Chem. B* **1999**, 103, 3292.
- Richmond, G. L. *Annu. Rev. Phys. Chem.* **2001**, 52, 257.
- Brown, M. G.; Walker, D. S.; Raymond, E. A.; Richmond, G. L. *J. Phys. Chem. B* **2003**, 107, 237.
- Becraft, K. A.; Moore, F. G.; Richmond, G. L. *J. Phys. Chem. B* **2003**, 107, 3675.
- Perry, A.; Ahlborn, H.; Space, B.; Moore, P. B. *J. Chem. Phys.* **2003**, 118, 8411.
- Lu, R.; Gan, W.; Wu, B. H.; Chen, H.; Wang, H. F. *J. Phys. Chem. B* **2004**, 108, 7297.
- Harris, A. L.; Rothberg, L. *J. Chem. Phys.* **1991**, 94, 2449.
- Kuhnke, K.; Morin, M.; Jakob, P.; Levinos, N. J.; Chabal, Y. J.; Harris, A. L. *J. Chem. Phys.* **1993**, 99, 6114.
- Bonn, M.; Hess, C.; Funk, S.; Miners, J. H.; Persson, B. N. J.; Wolf, M.; Ertl, G. *Phys. Rev. Lett.* **2000**, 84, 4653.
- Hess, C.; Wolf, M.; Roke, S.; Bonn, M. *Surf. Sci.* **2002**, 502, 304.
- Bonn, M.; Hess, C.; Roeterdink, W. G.; Ueba, H.; Wolf, M. *Chem. Phys. Lett.* **2004**, 388, 269.
- Hommel, E. L.; Ma, G.; Allen, H. C. *Anal. Sci.* **2001**, 17, 1325.
- Bordenyuk, A. N.; Benderskii, A. V. *J. Chem. Phys.* **2005**, 122, 134713.
- Whitnell, R. M.; Wilson, K. R.; Hynes, J. T. *J. Chem. Phys.* **1992**, 96, 5354.
- Stratt, M.; Maroncelli, M. *J. Phys. Chem.* **1996**, 100, 12981.
- Ladanyi, B. M.; Stratt, R. M. *J. Chem. Phys.* **1999**, 111, 2008.
- Benjamin, I. *Annu. Rev. Phys. Chem.* **1997**, 48, 401.
- Benjamin, I. Molecular dynamics of chemical reactions at liquid interfaces. In *Molecular Dynamics: From Classical to Quantum Methods*; Balbuena, P. B.; Seminario, J. M., Eds.; Elsevier: Amsterdam, 1999; p 661.
- Mitrinovic, D. M.; Tikhonov, A. M.; Li, M.; Huang, Z.; Schlossman, M. L. *Phys. Rev. Lett.* **2000**, 85, 582.
- Senapati, S.; Berkowitz, M. L. *Phys. Rev. Lett.* **2001**, 87, 176101.
- Schlossman, M. L. *Curr. Opin. Colloid Interface Sci.* **2002**, 7, 235.
- Wang, H.; Borguet, E.; Eisenthal, K. B. *J. Phys. Chem.* **1997**, 101, 713.
- Wang, H. F.; Borguet, E.; Eisenthal, K. B. *J. Phys. Chem. B* **1998**, 102, 4927.
- Michael, D.; Benjamin, I. *J. Chem. Phys.* **1997**, 107, 5684.
- Michael, D.; Benjamin, I. *J. Phys. Chem.* **1998**, 102, 5154.
- Steel, W. H.; Walker, R. A. *Nature* **2003**, 424, 296.
- Zhang, X.; Steel, W. H.; Walker, R. A. *J. Phys. Chem. B* **2003**, 107, 3829.
- Steel, W. H.; Walker, R. A. *J. Am. Chem. Soc.* **2003**, 125, 1132.
- Benjamin, I. *Chem. Rev.* **1996**, 96, 1449.
- Liu, P.; Harder, E.; Berne, B. J. *J. Phys. Chem. B* **2005**, 109, 2949.
- Benjamin, I. *J. Phys. Chem. B* **2005**, 109, 13711.
- Grubb, S. G.; Kim, M. W.; Raising, T.; Shen, Y. R. *Langmuir* **1988**, 4, 452.
- Eisenthal, K. B. *Chem. Rev.* **1996**, 96, 1343.
- Chandler, D. *Introduction to Modern Statistical Mechanics*; Oxford University Press: Oxford, 1987.
- Gai, H.; Voth, G. A. *J. Chem. Phys.* **1993**, 99, 740.
- Skinner, J. L.; Park, K. *J. Phys. Chem. B* **2001**, 105, 6716.
- Ryckaert, J. P.; Ciccotti, G.; Berendsen, H. J. C. *J. Comput. Phys.* **1977**, 23, 327.
- Zwanzig, R. *Annu. Rev. Phys. Chem.* **1965**, 16, 67.
- Landau, L.; Teller, E. *Z. Sowjetunion* **1936**, 10, 34.
- Bader, J. S.; Berne, B. J. *J. Chem. Phys.* **1994**, 100, 8359.
- Skinner, J. L. *J. Chem. Phys.* **1997**, 107, 8717.
- Allen, M. P.; Tildesley, D. J. *Computer Simulation of Liquids*; Clarendon: Oxford, 1987.
- Johnson, A. E.; Levinger, N. E.; Barbara, P. F. *J. Phys. Chem.* **1992**, 96, 7841.
- Kliner, D. A. V.; Alfano, J. C.; Barbara, P. F. *J. Chem. Phys.* **1993**, 98, 5375.
- Shiang, J. J.; Liu, H.; Sension, R. J. *J. Chem. Phys.* **1998**, 109, 9494.
- Benjamin, I.; Whitnell, R. M. *Chem. Phys. Lett.* **1993**, 204, 45.
- Batista, V. S.; Coker, D. F. *J. Chem. Phys.* **1997**, 106, 7102.
- Rowlinson, J. S.; Widom, B. *Molecular Theory of Capillarity*; Clarendon: Oxford, 1982.
- Benjamin, I. *J. Chem. Phys.* **2004**, 121, 10223.
- Chorny, I.; Vieceli, J.; Benjamin, I. *J. Chem. Phys.* **2002**, 116, 8904.
- Vieceli, J.; Chorny, I.; Benjamin, I. *J. Chem. Phys.* **2002**, 117, 4532.

- (85) Viecelli, J.; Chorny, I.; Benjamin, I. *Chem. Phys. Lett.* **2002**, 364, 446.
- (86) Chorny, I.; Viecelli, J.; Benjamin, I. *J. Phys. Chem. B* **2003**, 107, 229.
- (87) Chorny, I.; Benjamin, I. *J. Mol. Liq.* **2004**, 110, 133.
- (88) Winter, N.; Benjamin, I. *J. Chem. Phys.* **2004**, 121, 2253.
- (89) Hansen, J.-P.; McDonald, I. R. *Theory of Simple Liquids*, 2nd ed.; Academic: London, 1986.
- (90) Kuchitsu, K.; Morino, Y. *Bull. Chem. Soc. Jpn.* **1965**, 38, 814.
- (91) Benjamin, I. *J. Chem. Phys.* **1995**, 103, 2459.
- (92) Benjamin, I. Molecular dynamics simulations in interfacial electrochemistry. In *Modern Aspects of Electrochemistry*; Bockris, J. O. M., Conway, B. E., White, R. E., Eds.; Plenum Press: New York, 1997; Vol. 31; p 115.
- (93) Sprik, M.; Klein, M. L. *J. Chem. Phys.* **1988**, 89, 7556.
- (94) Ahlstrom, P.; Wallqvist, A.; Engstrom, S.; Jonsson, B. *Mol. Phys.* **1989**, 68, 563.
- (95) Wallqvist, A. *Chem. Phys.* **1990**, 148, 439.
- (96) Dang, L. X.; Rice, J. E.; Caldwell, J.; Kollman, P. A. *J. Am. Chem. Soc.* **1991**, 113, 2481.
- (97) Smith, D. E.; Dang, L. X. *J. Chem. Phys.* **1994**, 100, 3757.
- (98) Bader, J. S.; Berne, B. J. *J. Chem. Phys.* **1996**, 104, 1293.
- (99) Morita, A.; Kato, S. *J. Chem. Phys.* **1998**, 109, 5511.
- (100) Small, D. W.; Matyushov, D. V.; Voth, G. A. *J. Am. Chem. Soc.* **2003**, 125, 7470.
- (101) Wallqvist, A. *Chem. Phys. Lett.* **1990**, 165, 437.
- (102) Motakabbir, K.; Berkowitz, M. *Chem. Phys. Lett.* **1991**, 176, 61.
- (103) Chang, T. M.; Dang, L. X. *J. Chem. Phys.* **1996**, 104, 6772.
- (104) Benjamin, I. *Chem. Phys. Lett.* **1998**, 287, 480.
- (105) Dang, L. X.; Chang, T. *J. Phys. Chem. B* **2002**, 106, 235.
- (106) Jungwirth, P.; Tobias, D. J. *J. Phys. Chem. A* **2002**, 106, 379.
- (107) Xu, H.; Stern, H. A.; Berne, B. J. *J. Phys. Chem. B* **2002**, 106, 2054.
- (108) Benjamin, I.; Barbara, P. F.; Gertner, B. J.; Hynes, J. T. *J. Phys. Chem.* **1995**, 99, 7557.
- (109) Benjamin, I. *Faraday Discuss. Chem. Soc.* **2005**, 129, 47.
- (110) Li, M.; Owrutsky, J.; Sarisky, M.; Culver, J. P.; Yodh, A.; Hochstrasser, R. M. *J. Chem. Phys.* **1993**, 98, 5499.
- (111) Walhout, P. K.; Alfano, J. C.; Thakur, K. A. M.; Barbara, P. F. *J. Phys. Chem.* **1995**, 99, 7568.
- (112) Pohorille, A.; Wilson, M. A. *J. Mol. Struct. (THEOCHEM)* **1993**, 103, 271.
- (113) Reichardt, C. *Chem. Rev.* **1994**, 94, 2319.
- (114) Benjamin, I. *J. Phys. Chem. A* **1998**, 102, 9500.
- (115) Lee, L. T.; Langevin, D.; Mann, E. K.; Farnoux, B. *Physica B* **1994**, 198, 83.
- (116) Winter, N.; Benjamin, I. *J. Phys. Chem. B* **2005**, 109, 16421.
- (117) Oxtoby, D. W. *Adv. Chem. Phys.* **1979**, 40, 1.
- (118) Bizot, P.; Echargui, M. A.; Marsault, J. P.; Marsaultherail, F. *Mol. Phys.* **1993**, 79, 489.
- (119) Schvaneveldt, S. J.; Loring, R. F. *J. Chem. Phys.* **1996**, 104, 4736.
- (120) Ribeiro, M. C. C.; Santos, P. S. *J. Mol. Liq.* **1997**, 71, 25.
- (121) Kirkwood, J. C.; Ulness, D. J.; Albrecht, A. C. *Chem. Phys. Lett.* **1998**, 293, 167.
- (122) Tominaga, K.; Yoshihara, K. *J. Phys. Chem.* **1998**, 102, 4222.
- (123) Gayathri, N.; Bagchi, B. *Phys. Rev. Lett.* **1999**, 82, 4851.
- (124) Williams, R. B.; Loring, R. F. *J. Chem. Phys.* **1999**, 110, 10899.
- (125) Egorov, S. A.; Skinner, J. L. *J. Phys. Chem.* **2000**, 104, 483.
- (126) Wang, Z. H.; Wasserman, T.; Gershgoren, F.; Ruhman, S. *J. Mol. Liq.* **2000**, 86, 229.
- (127) Stenger, J.; Madsen, D.; Hamm, P.; Nibbering, E. T. J.; Elsaesser, T. *Phys. Rev. Lett.* **2001**, 8702, 7401.
- (128) Gershgoren, E.; Wang, Z. H.; Ruhman, S.; Vala, J.; Kosloff, R. *J. Chem. Phys.* **2003**, 118, 3660.